

1 NEUROMECHANICS OF MUSCLE SYNERGIES DURING CYCLING 2 - PROJECT REPORT*

3 SOPHIE HOARE[†]

4 **Abstract.** Throughout this report, the article *Neuromechanics of Muscle Synergies During*
5 *Cycling* [1] is revisited with the attempt to make new inferences from the data collected during the
6 2008 trial. The underlying goal of the original trial was to study "the extent to which synergistic
7 patterns of muscle activity vary when the mechanical demands on a limb were altered". Based on
8 new examinations of the data, this report attempts to answer if it is possible to determine the activity
9 condition from the relative phase advance of the Rectal femoris muscle from the Vastus medialis and
10 the Vastus lateralis muscles for an individual pedal cycle.

11 **1. Introduction.** For the 2008 journal article on muscle synergies during cycling
12 [1], Dr. James Wakeling, and visiting researcher Tamara Horn, conduct an experi-
13 mental trial with nine trained cyclists. They measure electrical activity (EMG) in
14 three main synergistic groups of muscles in one leg (ankle extensors, knee extensors
15 and knee flexors) while cycling on a stationary dynamometer for nine separate condi-
16 tions. These conditions included varying cadences and torques, varying the speed the
17 cyclist must pedal, or rather the force applied, respectively, while completing 24 pedal
18 revolutions. With a focus on muscle synergies (groups of muscles that are recruited
19 in a coordinated fashion with coherent activations), their aim was to test two main
20 hypotheses:

- 21 1. that a significant ($> 10\%$) proportion of the patterns of activity is modulated
22 due to the movement mechanics (the load and velocity required during the
23 task), and
- 24 2. that activity of muscles within an anatomic group would show a significant
25 ($> 10\%$) uncoupling when the limb was challenged with a range of mechanical
26 conditions.

27 The use of the term *pattern of activity* within the text is described as referring
28 to "the relative levels of activation that can occur across a set of muscles at a set
29 moment in time" [1]. Also described is, that, a pattern of activation could correspond
30 to a muscle synergy required to complete the task, but could also refer to synergies
31 that have been modulated by feedback. There is no way to distinguish between the
32 two, thus, the authors focus on "time-varying patterns of the levels of EMG across
33 groups of muscles" [1].

34 This paper is organized as follows: First, we take a deep dive into the properties of
35 the data set in section 2. Then, the problem statement is introduced in section 3. The
36 main algorithms used, and tests conducted, are described in section 4 and section 5.
37 This is followed by experimental results in section 6. The report is then concluded
38 with a brief summary in section 7.

39 **2. Properties of the Data.** As described above, the experiment was conducted
40 with nine cyclists. All cyclists were male, aged between 31 and 37, with a mass
41 between 71.7 kg and 80.5 kg, and a height between 1.77 m and 1.81 m. The test
42 conditions were: 60, 80, 100, 120, or 140 rpm at a crank torque of 6.5 N m and
43 additionally crank torques of 12.9, 25.1, 32.4, and 39.9 N m at a pedal cadence of 60
44 rpm. To minimize possible bias within the trials (e.g. fatigue of muscles), the subjects

*Simon Fraser University, APMA 920: Numerical Linear Algebra, Fall 2022

[†]Applied Mathematics Graduate Student at SFU (sgh6@sfu.ca, <https://github.com/shoare55/SFU-APMA920-Term-Project>).

spent 5 minutes warming up, then the experimental conditions were presented in a randomized block fashion with 45 seconds of rest between conditions. Data was recorded for 30 seconds of steady cycling at each condition. The EMG intensities were calculated for 28 pedal cycles per trial and sub-divided into 100 equally spaced time windows. The data was then normalized to the mean of the total intensities for all spectra across all trials.

Wakeling and Horn [1] use principal component analysis to characterize the EMG signals. The PC weights were determined from the covariance matrix of the true data. At the end of their trial, Wakeling and Horn evaluated heart rate correlation, mean EMG signal correlation, and activation patterns in relation to the variations in crank torque and pedal cadence. As they expected, heart rate showed a significant correlation to the required mechanical power output needed for a particular condition. They also noted that there was no significant difference between the three blocks of the trial, indicating that their protocol to remove bias aligned with the desired effect on heart rate. The mean EMG signal showed the lowest values for the condition with the lowest mechanical power output of 60 rpm and 6.5 N m. This increased with both increases in crank torque and pedal cadence. With this being said, they found that the mean intensities with varied conditions differed between muscles. Each group of muscle synergies had their own corresponding intensities per condition. Eventually, they determined that the activity of muscles within anatomic groups was only partially uncoupled in response to altered mechanical demands on the limb.

One key observation in their results was focused on the quadriceps muscles. They noted that the Rectal femoris (RF) showed a significant phase advance compared to the Vastus medialis (VM) and the Vastus lateralis (VL) for high cadence trials. These muscles are members of the knee extensors anatomic group with the main function being to extend the leg at the knee. It was noted that, at the highest crank torque, the mean EMG intensity of the RF showed greater activity than the VM and VL. This observation is what drives the problem statement for this project.

3. Problem Statement. Throughout this report, the problem addressed is:

Can we determine the condition of a pedal cycle based on the relative phase advance of the Rectal femorus (RF) from the Vastus medialis (VM) and the Vastus lateralis (VL) muscles in the raw EMG traces.

This problem can be directly related to the second hypothesis of the original paper. As the mechanical power required increases, we expect to see the activations with the quadriceps differ. For the purpose of this report, we focus on using phase advances to reflect such differences. Therefore, it is required to determine if the significance of the uncoupling in the knee extensors can be directly correlated to the observed phase advances. That is, can we link how early the RF is recruited for an activity (in comparison to the VM and VL) to the related trial condition?

The original paper breaks down the relative uncoupling of the quadriceps using varimax patterns. The use of varimax rotation allows the simplification of the expression for a particular sub-space, such as the sub-space found with principal component analysis. Wakeling and Horn state that 23.4% of the EMG intensities corresponded to an uncoupling of the RF from the VM and VL. The uncoupling can be seen in varimax patterns III-VI. In an attempt to address the related phase analysis problem stated in this report, we use cross-correlation between the raw activation of the RF from the VM and VL, as well as correlation matrices between the test data and the average training data to predict trial conditions.

4. Mathematical Algorithms. Throughout this section is a description of the two main tools used to evaluate the phase advance of Rectal femoris from the Vastus medialis and the Vastus lateralis along with an algorithm to compare test samples against the training data.

The two key techniques applied are correlation and cross-correlation of time series. A correlation coefficient is a direct measure of linear dependence between two random variables, whereas cross-correlation is a measure of similarity between two series describing the displacement of one relative to the other. The cross-correlation is key in analyzing the relative phase advance of the RF at each condition, and the Pearson correlation coefficient is essential in determining which condition best matches the test sample.

DEFINITION 1 (Pearson Correlation Coefficient). *The population correlation coefficient $\rho_{X,Y}$ between two random variables X and Y with expected values μ_X and μ_Y and standard deviations σ_X and σ_Y is defined as:*

$$\rho_{X,Y} = \mathbf{corr}(X,Y) = \frac{\mathbf{cov}(\mathbf{X}, \mathbf{Y})}{\sigma_X \sigma_Y} = \frac{E[(X - \mu_X)(Y - \mu_Y)]}{\sigma_X \sigma_Y}, \text{ if } \sigma_X \sigma_Y > 0$$

where E is the expected value operator, \mathbf{cov} means covariance, and \mathbf{corr} is a widely used alternative notation for the correlation coefficient.

Within Matlab, the command used for correlation coefficients is `corrcoef(A,B)`. It is defined by

$$\rho(A,B) = \frac{1}{N-1} \sum_{i=1}^N \left(\frac{A_i - \mu_A}{\sigma_A} \right) \left(\frac{B_i - \mu_B}{\sigma_B} \right)$$

where N is the number of scalar observations.

DEFINITION 2 (Cross-correlation). *Let (X_t, Y_t) be a pair of random processes, and t be any point in time (t may be an integer for a discrete-time process or a real number for a continuous-time process). Then X_t is the value (or realization) produced by a given run of the process at time t . Suppose that the process has means $\mu_X(t)$ and $\mu_Y(t)$ and variances $\sigma_X^2(t)$ and $\sigma_Y^2(t)$ at time t , for each t . Then the definition of the cross-correlation between times t_1 and t_2 is*

$$R_{XY}(t_1, t_2) \triangleq E[X_{t_1} Y_{t_2}]$$

where E is the expected value operator.

Within Matlab, the command used for cross-correlation is `xcorr(x,y)`. It is defined by

$$\hat{R}_{XY}(m) = \begin{cases} \sum_{n=0}^{N-m-1} x_{n+m} y_n^*, & m \geq 0 \\ \hat{R}_{YX}(-m), & m < 0 \end{cases}$$

with output vector, c , with elements given by

$$c(m) = \hat{R}_{XY}(m - N), \quad m = 1, 2, \dots, 2N - 1$$

In order to produce an accurate estimate for the cross-correlation between two muscle EMG signals for an individual pedal cycle, normalization was also required.

Upon extracting the training data set, the mean RF vector and mean VM & VL vector is produced. The cross-correlation vector is then determined for each condition. These nine vectors are then used to make predictions via the following algorithm in [Algorithm 1](#).

Algorithm 1 Make Prediction

Input: T , an (m, n) matrix of test data, $C = \{\{c_1\}, \dots, \{c_t\}\}$, a cell with 9 averaged cross-correlation vectors for each condition, and $C_{map} = \{\hat{c}_1, \dots, \hat{c}_t\}$, a vector with 9 condition maps for each cell in C .

Extract RF and $V_{M\&L}$ the average of VL and VM muscles from T .

Initialize predictions vector P

for $j = 1 : m$ **do**

 Compute normalized $T_j := \mathbf{xcorr}(RF, V_{M\&L})$

 Initialize correlation vector X

for $k = 1 : 9$ **do**

 Extract $C_k :=$ cross-correlation vector k from C

 Compute $X_k = \mathbf{corrcoef}(T_j, C_k)$

end for

 Set $P_j = C_{map}(m)$, the m 'th entry in C_{map} where $X_m = \max(X)$

end for

return P

5. Experimental Tests. As noted in Wakeling and Horn's findings, the Rectal femoris showed a significant phase advance compared to the Vastus medialis (VM) and the Vastus lateralis (VL) for high cadence trials. We can observe the extent of this in Figure 1. From the raw EMG signals we can see clearly the average over the VM and VL muscle behaves differently than the RF muscle. We observe similar patterns at conditions 60 rpm with 6.5 N m and 12.5 N m crank torques, at 60 rpm

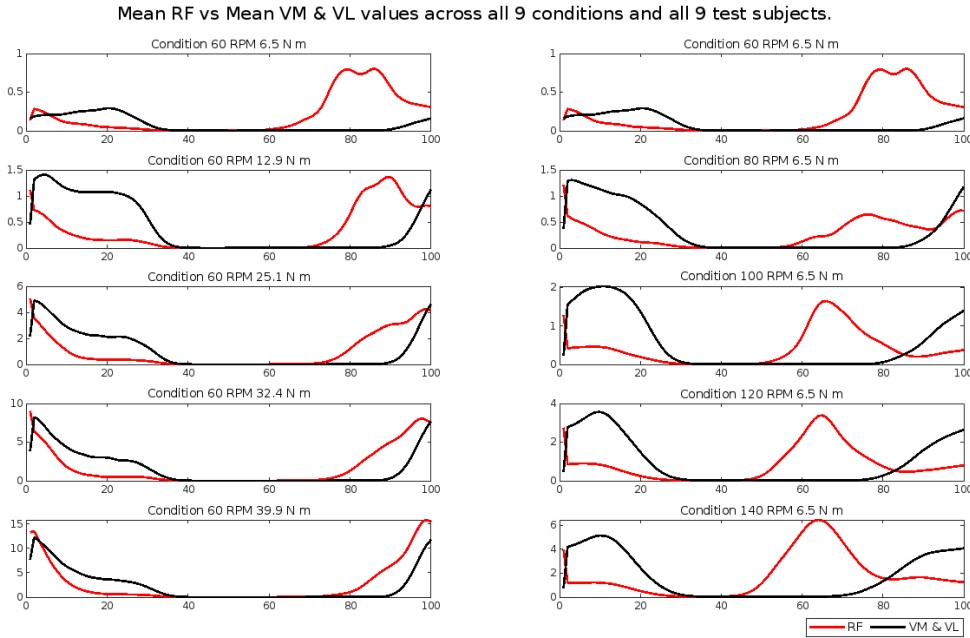


FIG. 1. Plot of the mean normalized EMG signal for RF muscle and VM and VL muscles combined over all subjects and all conditions.

with 25.1 N m, 32.4 N m and 6.5 N m crank torques, and the group containing 100 rpm, 120 rpm and 140 rpm at 6.5 N m crank torque.

The cross-correlation vectors for the RF vs the mean VM and VL muscle in Figure 2 show similar grouping patterns. We see clear similarities between conditions 60 rpm with 6.5 N m and 12.5 N m crank torques. We also note, that, condition 80 rpm and 6.5 N m crank torque appears to be best matched to these two conditions also. The second grouping appears with conditions 60 rpm with 25.1 N m, 32.4 N m and 39.9 N m crank torques, and the last grouping being with the remaining conditions, 100 rpm, 120 rpm and 140 rpm at 6.5 N m crank torque.

Cross-Correlation Vector for RF muscle vs Mean VM & VL across all 9 conditions all 9 test subjects.

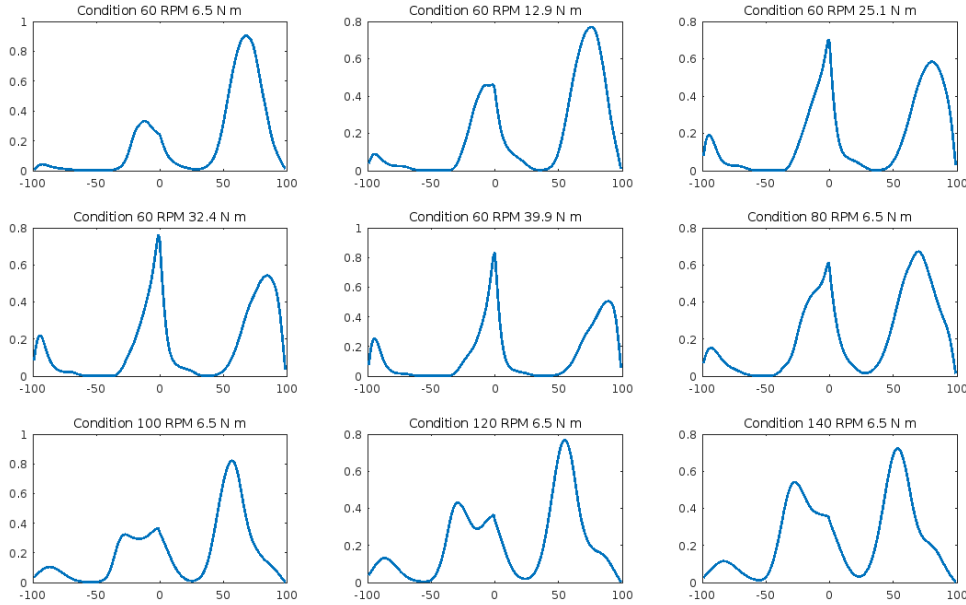


FIG. 2. Plot of the cross-correlation vector between the RF muscle and VM and VL muscles averaged over all subjects and all conditions.

With the original problem statement in mind, we define Experiment 1 in 5.1.

5.1. Experiment 1. The initial experiment is to predict the true condition of the pedal cycle based on the normalized cross-correlation vector of the test sample's RF raw EMG signals with the average of the VM and VL raw EMG signals. Note that each pedal cycle is split into 100 equally spaced time windows as mentioned in section 2.

In order to try and remove any bias from the results, we redefine the training and testing set for each trial, for a total of 100 trials. For each trial, we remove one random subject from the data. We then take a random subset of the remaining 8 subjects based on the desired training percentage. E.g. training percentage of 70% means we randomly select 70% of the pedal cycles from the 8 subjects left and define this as our training set. We then average the RF muscle and the VM and VL muscles over all of the training data for each condition and compute the base cross-correlation vectors that will be used as input, C , for Algorithm 1 along with the appropriate mappings, C_{map} . We then define two separate testing sets of data. The first is test set A , which

includes the remaining data from the 8 subjects left after randomly removing one. E.g. with a training percentage of 70% as above, test set A will include the remaining 30% of that data. The second testing set, test set B , is defined as all data from the subject that was removed. It is our hope that the performance of Algorithm 1 is to predict the true conditions from test set A and test set B will be similar.

Due to the clear groupings that are observed in Figure 2 when we average over all the data, it is likely that the performance of this experiment may not be as accurate as desired. It is possible that Algorithm 1 may not successfully identify the condition of the pedal cycle, but rather predict one of the similar conditions due to variation between subjects.

In order to get a better understanding of the trends observed in Figure 2, we define matrix D as follows:

$$D_{i,j} = \text{corrcoef}(c_i, c_j) \text{ for } i, j = 1, \dots, 9$$

where c_n is the result of taking correlation coefficient between the average for the RF muscle and the VM and VL muscles over all of the training data for each condition n . The results can be seen in Figure 3.

Condition Of Trial	60 RPM 6.5 N m	60 RPM 12.9 N m	60 RPM 25.1 N m	60 RPM 32.4 N m	60 RPM 39.9 N m	80 RPM 6.5 N m	100 RPM 6.5 N m	120 RPM 6.5 N m	140 RPM 6.5 N m
60 RPM 6.5 N m	1	0.8918	0.6575	0.5338	0.3863	0.9057	0.7013	0.5682	0.5011
60 RPM 12.9 N m	0.8918	1	0.9068	0.8241	0.7005	0.935	0.4615	0.3384	0.2989
60 RPM 25.1 N m	0.6575	0.9068	1	0.9852	0.9326	0.8604	0.2993	0.2098	0.1799
60 RPM 32.4 N m	0.5338	0.8241	0.9852	1	0.9794	0.7839	0.2175	0.1426	0.1105
60 RPM 39.9 N m	0.3863	0.7005	0.9326	0.9794	1	0.6832	0.1413	0.0839	0.0487
80 RPM 6.5 N m	0.9057	0.935	0.8604	0.7839	0.6832	1	0.6987	0.5937	0.5475
100 RPM 6.5 N m	0.7013	0.4615	0.2993	0.2175	0.1413	0.6987	1	0.9718	0.9158
120 RPM 6.5 N m	0.5682	0.3384	0.2098	0.1426	0.0839	0.5937	0.9718	1	0.9753
140 RPM 6.5 N m	0.5011	0.2989	0.1799	0.1105	0.0487	0.5475	0.9158	0.9753	1

FIG. 3. Matrix D , the correlation matrix between all cross-correlation vectors for the RF muscle and the VM and VL muscles over all data for each condition.

The easiest block to identify occurs in the bottom right corner of matrix D , indicating the high correlation between conditions 100 rpm, 120 rpm and 140 rpm at 6.5 N m crank torque. All of the correlation coefficients are above 0.9 confirming our earlier observation of their similarities. The second block identified is slightly less clear and occurs in the center of matrix D . The corresponding conditions are 60 rpm at 25.1 N m, 32.4 N m, and 39.9 N m crank torques. The reason this block is harder to identify is because condition 2, 60 rpm with 12.9 N m crank torque, also has a high correlation to condition 60 rpm with 25.1 N m crank torque. The last group that we identified earlier on in the report based on observations in Figure 2 included 60 rpm with 6.5 N m and 12.9 N m crank torques, and 80 rpm at 6.5 N m crank torque. This group is confirmed in matrix D with correlation coefficients all above 0.9.

Based on the clear grouping of conditions, we proceed by defining Experiment 2 in 5.2 and Experiment 3 in 5.3.

5.2. Experiment 2. As in 5.1, we define our training and test sets in the same manner, excluding one subject and taking a certain percentage for training with the remaining being used for testing. We then average the RF muscle and the VM and VL muscles over all of the training data for each condition and compute the base cross-correlation vectors that will be used as input, C , for Algorithm 1. In contrast to Experiment 1 in 5.1, we define C_{map} based on the corresponding condition grouping

identified above. These groups are defined by:

- Group 1 : $\{c_1 = 60 \text{ rpm and } 6.5 \text{ N m}, c_2 = 60 \text{ rpm and } 12.9 \text{ N m},$
 $c_6 = 80 \text{ rpm and } 6.5 \text{ N m}\}$
- Group 2 : $\{c_3 = 60 \text{ rpm and } 25.1 \text{ N m}, c_4 = 60 \text{ rpm and } 32.4 \text{ N m},$
 $c_5 = 60 \text{ rpm and } 39.9 \text{ N m}\}$
- Group 3 : $\{c_7 = 100 \text{ rpm and } 6.5 \text{ N m}, c_8 = 120 \text{ rpm and } 6.5 \text{ N m},$
 $c_9 = 140 \text{ rpm and } 6.5 \text{ N m}\}$

Predictions are then made for test set A and test set B based on the condition group number. Due to the nature of the cross-correlation vectors across all data, we expect the accuracy of the predictions to be much higher than in Experiment 1.

5.3. Experiment 3. In Experiment 3, we complete the exact same process for creating the training and testing sets, and computing the cross-correlation vectors stored in C . However, this is not what we input into Algorithm 1. Instead, we create a smaller set, C_{new} , defined by taking the average of the cross-correlation vectors in each group. The groups used in Experiment 3 are defined slightly differently than in Experiment 2, in order to try and take into consideration the high correlation between conditions 60 rpm and 12.9 N m crank torque and 60 rpm and 25.1 N m crank torque. We do this by including condition 2 (60 rpm and 12.9 N m crank torque) in both Group 1 and Group 2. Thus, we define $C_{new} = \{\{\tilde{c}_1\}, \{\tilde{c}_2\}, \{\tilde{c}_3\}\}$ with

$$\begin{aligned}\tilde{c}_1 &= \text{mean}(c_1, c_2, c_6) \\ \tilde{c}_2 &= \text{mean}(c_2, c_3, c_4, c_5) \\ \tilde{c}_3 &= \text{mean}(c_7, c_8, c_9)\end{aligned}$$

and $\tilde{C}_{map} = \{\hat{c}_1, \hat{c}_2, \hat{c}_3\}$. Predictions are then made via Algorithm 1 using C_{new} and \tilde{C}_{map} . It is expected that the accuracy of the predictions for Experiment 3 is similar to Experiment 2, with possibly a slight improvement

6. Main results. Experiments 1, 2 and 3 are completed a total of 100 times at training percentages 0.6, 0.7, and 0.8 respectively. The results are as shown in Figure 4, Figure 5 and Figure 6. At first glance, it is clear that the behaviour with training percentages 0.6, 0.7 and 0.8 the accuracy trends are similar. Looking at Figure 4, the results for test set A with Experiment 1 fluctuate between 0.3 accuracy and 0.4 accuracy of predictions. We have an average accuracy of approximately 0.34. As expected, the result for Experiment 2 and Experiment 3 is greatly improved. There is a clear improvement of approximately 0.4 on average. Both Experiments 2 and 3 fluctuate between 0.67 and 0.76 accuracy with an average of approximately 0.71 and 0.72 respectively.

Similarly, test set B has a large improvement in average accuracy between Experiments 1, 2 and 3. In contrast, when observing the accuracy for test set B over all trials with all experiments, the accuracy fluctuates greatly. The accuracy for Experiment 1 has a range between 0.1 and 0.55, and Experiments 2 and 3 have a range between 0.32 and 0.94. Although this is an extremely large range, the average for both experiments is towards the higher of this range. For Experiments 2 and 3, the average is approximately 0.71. Based on this, it is my assumption that 1 or 2 of the subjects are those that are causing the low accuracy predictions. It is likely that these

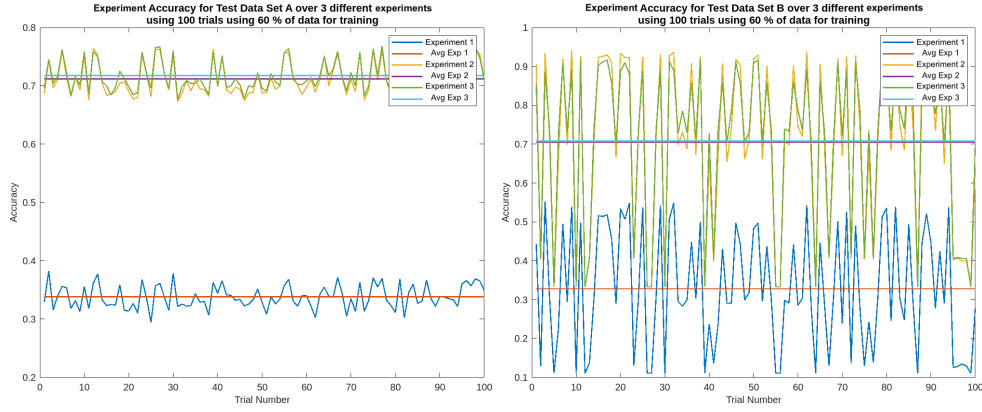


FIG. 4. Accuracy results for test set A (left) and test set B (right) with 60% training percentage over 100 trials.

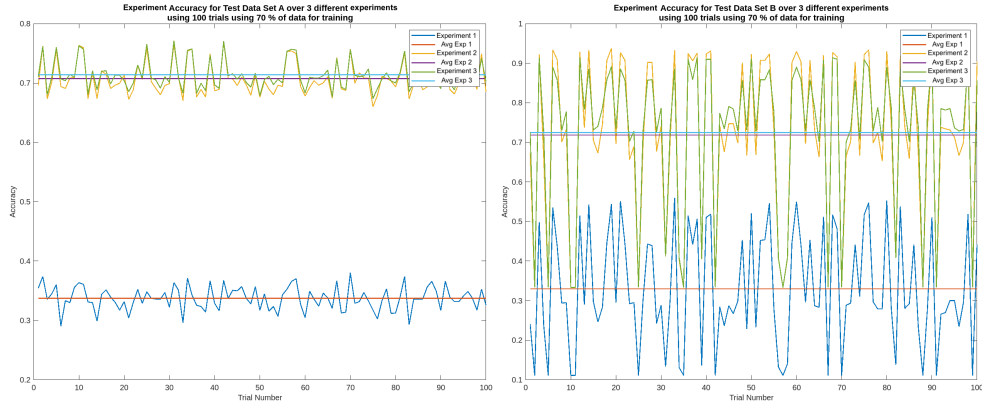


FIG. 5. Accuracy results for test set A (left) and test set B (right) with 70% training percentage over 100 trials.

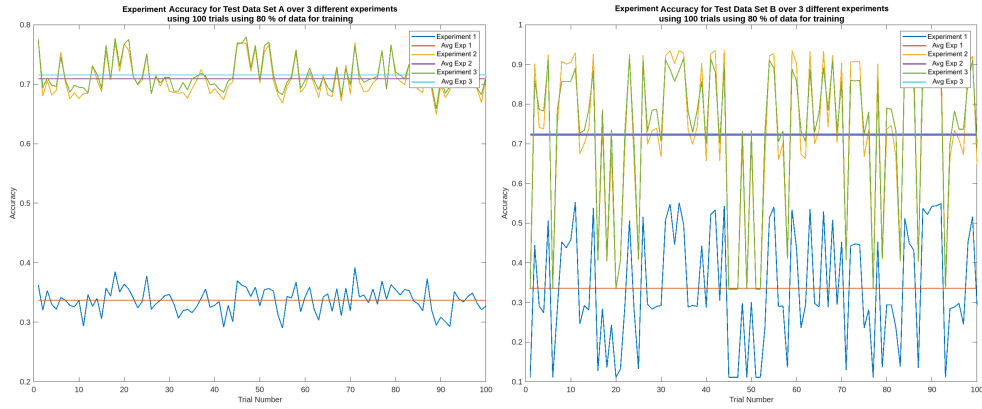


FIG. 6. Accuracy results for test set A (left) and test set B (right) with 80% training percentage over 100 trials.

subjects have a different activation pattern of the RF to the VM and VL due to a physical difference in the way that their muscles work together to complete the task across all conditions.

When the training percentage is increased to 0.7 and 0.8, the results trend in a very similar fashion. For test set *A* with training percent 0.7, we see that Experiment 1 has a mean accuracy of approximately 0.34 with minor fluctuations over the 100 trials. Experiments 2 and 3 both have mean accuracy of approximately 0.71, also with minor fluctuations. For test set *B* with training percent 0.7, we see that Experiment 1 has a mean accuracy of 0.33 and fluctuations up to ± 0.24 . Experiments 2 and 3 both have a mean accuracy of approximately 0.72 with fluctuations up to ± 0.39 . For test set *A* with training percent 0.8, we see that Experiment 1 again has a mean accuracy of approximately 0.34 with minor fluctuations over the 100 trials. Experiment 2 has a mean of approximately 0.71, and Experiment 3 has a mean accuracy of approximately 0.72, also with minor fluctuations. For test set *B* with training percent 0.8, we see that Experiment 1 has a mean accuracy of 0.34 and fluctuations up to ± 0.24 . Experiment 2 has a mean accuracy of approximately 0.72 and Experiment 3 has the greatest mean accuracy of approximately 0.73 with fluctuations that drop down to the mean accuracy line of Experiment 1 at 0.34.

Along with running the three experiments at training percentages 0.6, 0.7 and 0.8, I also completed the experiments for training percentages from 0.2 to 0.95 increasing by 0.05 each iteration. At all training percentages, 100 trials were completed and the mean accuracy was recorded. Figure 7 shows the results for Experiment 1 and Figure 8 shows the results for Experiments 2 and 3. In Figure 7, data set *A* has minimal fluctuations no matter the percentage of training data used. At training percent 0.2, there is a total of 1206 data rows for training, and Algorithm 1 must predict a total of 4842 pedal cycle conditions. At training percent 0.95, there is a total of 5742 data rows for training, and Algorithm 1 only needs to predict a total of 306 pedal cycle conditions.

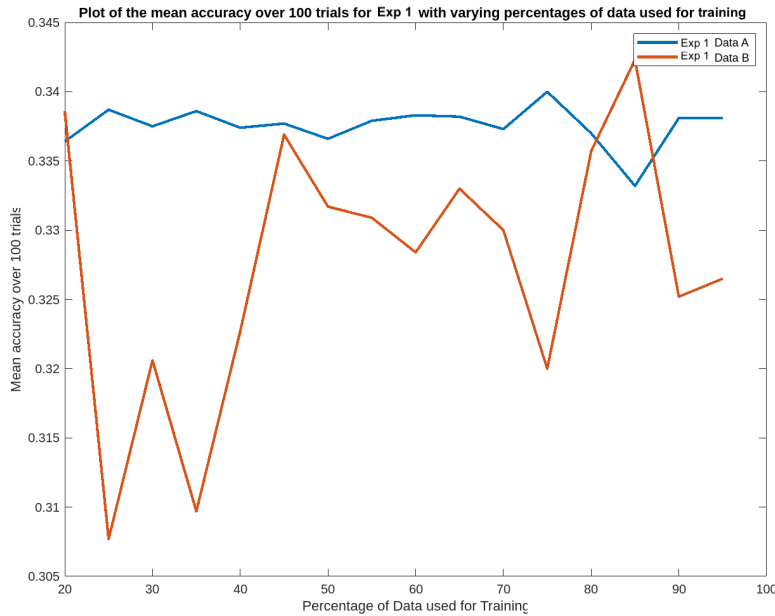


FIG. 7. Mean accuracy over 100 trials for increasing training percentage for Experiment 1.

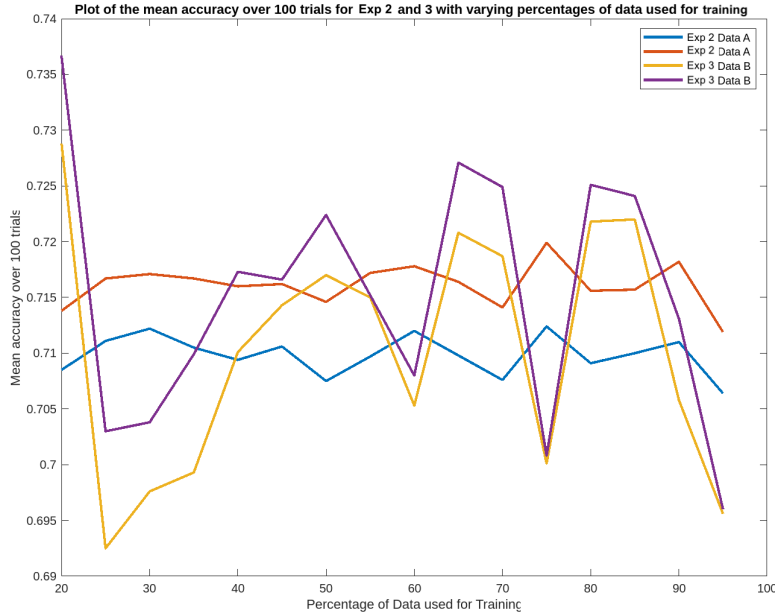


FIG. 8. Mean accuracy over 100 trials for increasing training percentage for Experiment 2 and 3.

Although this is true, the mean accuracy between 0.2 and 0.7 barely fluctuates and stays at approximately 0.337. In contrast, data set *B* must predict a total of 756 pedal cycle conditions no matter the training percent, and there is a much greater fluctuation between the mean accuracy over 100 trials at each training percentage. We see that at 0.25 and 0.35 training percentages, there is an extreme low of approximately 0.31 mean accuracy. As the training percentage increases, it appears as though there is an upward trend in the mean accuracy.

In Figure 8, we see the trends for both Experiment 2 and Experiment 3 follow the same pattern when we split it into data set *A* and data set *B*. As stated above, at training percent 0.2 the model only has 1206 data rows for training and must predict 4842 pedal cycle condition groups. At training percent 0.95 the model has 5742 data rows for training and only needs to predict 306 pedal cycle conditions. Similar to Experiment 1, data set *B* has a low at training percent 0.25. It ranges from 0.69 to 0.735 in accuracy across all training percentages. Also, data set *A* follows a similar trend to Experiment 1 with only minor fluctuations with Experiment 2 around 0.71 and Experiment 3 around 0.715. Overall, the training percentage does not seem to have a large impact on the mean prediction accuracy, indicating that the cross-correlation vectors at each condition remain to be a good representation of the data even with a small data set.

7. Summary. In order to address the problem statement of determining the condition of a pedal cycle based on the relative phase advance of the Rectal femorus from the Vastus medialis and the Vastus lateralis using the raw EMG traces, three experiments were designed and conducted. Due to clear correlations between 3 groups of conditions, determining the condition of a pedal cycle over all conditions was relatively unsuccessful for both a subset of test subjects included in training (test set *A*), and for unseen test subject data (test set *B*) with accuracy trending around 30%.

Once conditions were grouped in Experiments 2 and 3, we see a great improvement for both test set A and test set B . The model is able to predict the pedal cycle condition group for both data types with an average of approximately 71% accuracy. Within the original paper, Wakeling and Horn [1] noted that the relative phase advance was more pronounced for the high cadence trials than the low cadence trials where the timing of the three muscles was much more closely matched. Throughout this report, we show that there are three groupings when comparing the timing of the three muscles and that we can predict the condition group from an individual pedal cycle based on the relative phase advance of the Rectal femorus muscle with around 70% confidence.

REFERENCES

- [1] J. M. WAKELING AND T. HORN, *Neuromechanics of muscle synergies during cycling*, Journal of Neurophysiology, 101 (2009), p. 843–854, <https://doi.org/10.1152/jn.90679.2008>.